Experimental band structure of 1 T-$TiSe_2$ in the normal and charge-density-wave phases

N. G. Stoffel,* S. D. Kevan, and N. V. Smith
AT&T Bell Laboratories, 600 Mountain Avenue, Murray Hill, New Jersey 07974
(Received 26 December 1984)

We have studied the charge-density-wave phase transition of $TiSe_2$ using photoelectron spectroscopy with high angle and energy resolution. We accurately measured the band dispersions of the Se $4p$ and Ti $3d$ bands, whose interaction is thought to be deeply involved in the phase transition. In contrast to the commonly held view that $TiSe_2$ has a semimetallic band structure with a substantial indirect band overlap, we report the existence of a small semiconducting gap for $TiSe_2$ in either phase. This has important implications for current efforts to establish a microscopic model of the charge-density-wave transition. At low temperatures the folding of the band structure which accompanies the formation of the charge-density-wave superlattice is seen directly in our photoemission spectra.

I. INTRODUCTION

The layered compound $1T-TiSe_2$ undergoes a $2a_0 \times 2a_0 \times 2c_0$ charge-density-wave (CDW) phase transition below 200 K which involves no intermediate incommensurate phase.[1] This strongly suggests that the commensurate charge-density-wave vector is locked in by an interaction between the Se $4p$ valence band maximum at the center of the Brillouin zone (Γ) and the pocket of Ti $3d$ states at the zone edge at L. These symmetry points are connected by the new reciprocal lattice vectors introduced by the CDW transition, and therefore become equivalent Γ points in the CDW state, allowing direct interaction of the p and d bands. Both an excitonic insulator mechanism[2] and a Jahn-Teller band instability model[3] have been proposed to explain in a qualitative fashion the nature of the CDW transition; both models explicitly involve the p-d interaction. Yoshida and Motizuki[4] have developed a quantitative microscopic model of the lattice instability based on the latter model. They calculate the electronic susceptibility of $TiSe_2$ taking into account the wave vector, temperature, and mode dependence of the electron-lattice interaction. The principle result of their work is a calculated temperature-dependent softening of a transverse phonon mode at the wave vector spanning Γ and L (L_1^-). The condensation of phonons in the three degenerate L_1^- modes at low temperature leads to a lattice distortion which is consistent with neutron-diffraction results.[1] The CDW model of Yoshida *et al.*[4] takes as a starting point the tight-binding band structure of Zunger and Freeman,[5] which exhibits an indirect p-d band overlap of 0.2 eV. Extending this work, Suzuki *et al.*[6] have calculated the electronic structure of $TiSe_2$ assuming this overlap obtains for the normal phase. In the CDW phase they find a strong p-d interaction near the Fermi energy which opens up a gap of about 0.2 eV over a large volume of the Brillouin zone.

Photoemission studies[7–9] have suggested that the CDW transition is indeed accompanied by changes in the electronic structure of the p and d bands in a narrow energy interval near the Fermi energy. Other transport and diffraction experiments[1,10,11] have been performed on $TiSe_2$ crystals in which the relative positions of the p and d bands and the Fermi energy were altered by doping or substitution. The results demonstrate that the CDW phase transition temperature depends sensitively on these parameters, and that the phase transition can be completely suppressed by shifting the p and d bands by a small fraction of an eV. Clearly, a full understanding of the CDW state of $TiSe_2$ requires an accurate determination of the p-d band lineups. Unfortunately, a consensus of the magnitude and sign of the p-d overlap has not been attained experimentally or theoretically. Early band-structure calculations[12] yielded a large (>1 eV) semiconductor band gap for $TiSe_2$, but a semimetallic band overlap (up to 0.6 eV) was reported in later works.[5,13] Recently, von Boehm and Isomäki[14] calculated the relative p-d positions including relativistic corrections, and they found a 0.24 eV band gap. Experimentally determined band overlaps of roughly 1 eV,[15] 0.2 eV,[16] and 0.0 eV (Ref. 17) were reported in previous angle-resolved photoelectron spectroscopy (ARPES) studies by various groups.

We have performed high-resolution ARPES on $TiSe_2$ both at room temperature and at 77 K in order to determine its electronic structure near the Fermi energy more accurately and to search for changes accompanying the CDW phase transition. We took into account the effects of band dispersion perpendicular to the plane of the layers. By varying the photon energy for these experiments we are able to observe significant band dispersion along the c-axis in spite of the quasi-two-dimensional nature of $TiSe_2$. We find that the p and d bands do not overlap even at the extremes of this dispersion. Instead $TiSe_2$ appears to be a very narrow gap semiconductor such that the p and d bands can interact strongly over a smaller volume of the Brillouin zone than if it were a true semimetal.

The organization of this paper is as follows: In Sec. II we will discuss the experimental equipment and procedures. Room-temperature and low temperature angle-resolved photoemission results will be presented in Sec. III

and IV. A discussion of these results and their implications about the CDW transition appears in Sec. V.

II. EXPERIMENTAL PROCEDURES

These ARPES experiments were performed on a 6-m toroidal grating monochromator beam line[18] at the National Synchrotron Light Source. The photon-energy resolution was 50 meV or better for photon energies 10 eV $\leq \hbar\omega \leq$ 85 eV. A spherical deflector analyzer[19] on a two-axis goniometer was used to collect electron energy distribution curves with an overall energy resolution of better than 100 meV and an angular resolution of 1.3°.

A 5-mm-diam crystal of $TiSe_2$ was mounted on a Dewar and cleaved under vacuum to expose a smooth surface along the (0001) plane. The orientation of the sample was determined *in situ* by low-energy-electron diffraction and its cleanliness was checked by Auger spectroscopy. It was ascertained that the sample yielded identical spectral features over a sufficiently large area that contractions of the Dewar during cooldown would not produce changes in the ARPES spectra. The Dewar was filled with liquid nitrogen during the low-temperature experiments. The sample surface temperature was not measured directly but is referred to as 77 K in this paper.

The $TiSe_2$ crystal was grown by standard transport methods at a temperature chosen to promote ideal 1:2 stoichiometry. We observe a filling of the Ti $3d$ band over about 1% of the Brillouin zone but find no evidence for Se $4p$ holes, suggesting an excess of Ti which probably resides in the interstitial sites between the layers. Such excess Ti would act as a multivalent donor, raising the Fermi level substantially and filling part of the lowest Ti $3d$ band at L and removing any holes at Γ. In a rigid band model we expect only second-order effects from nonstoichiometry upon the relative p-d positions. A Lorentzian peak-fitting algorithm was used to determine precisely the relative energies, areas, and widths of the peaks found in the ARPES spectra.

III. ROOM-TEMPERATURE ARPES RESULTS

A principal contribution of this study to the determination of the relative p-d band positions in $TiSe_2$ is an accurate photon-energy-dependent measurement of the energy of the Se $4p$ band maximum. In all previous ARPES studies a set of Se $4p$ spectral features was seen near the Fermi level at normal emission. These features are much broader than the Ti $3d$ peaks which appear at higher emission angles, and they do not always exhibit simple dispersion patterns. These effects make it difficult to locate the valence-band maximum to better than a few tenths of an eV. We find that both these problems can be alleviated to a large extent by a choice of photon energy which excites transitions from initial states near Γ. In fact, the valence band maximum is probed only at such photon energies.

In Fig. 1 we present a series of room-temperature spectra collected at various polar angles θ using a photon energy of 18 eV. The azimuthal angle corresponds to a $\bar{\Sigma}$ direction of the surface Brillouin zone of $TiSe_2$. (The relationship between the surface and bulk Brillouin zones of the normal lattice and that of the reconstructed bulk lattice are illustrated in Fig. 2.) The sharp peaks near E_F in the spectra at angles near 30° arise from a pocket of Ti $3d$ electrons near L. The L point has a reciprocal lattice vector parallel to the surface $\mathbf{k}_{||}=2\pi/a_0\sqrt{3}=1.018$ Å^{-1} and projects onto the $\bar{M}$ point of surface lattice. Using the usual kinematic formula,

$$|\mathbf{k}_{||}| = (0.5123 \text{ Å}^{-1})\sin\theta(E_k)^{1/2}, \quad (1)$$

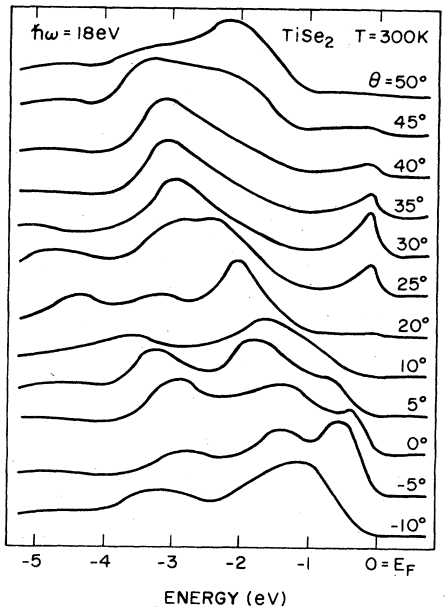

FIG. 1. Series of ARPES spectra collected from room-temperature $TiSe_2$ along the $\bar{\Sigma}$ azimuth using 18-eV photons. Ti $3d$ and Se $4p$ bands are both visible, but the dispersions of the latter are difficult to determine accurately at this and higher photon energy.

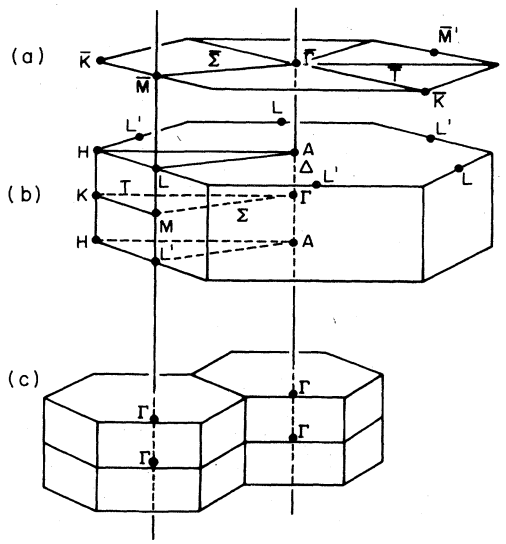

FIG. 2. Reciprocal lattices of $TiSe_2$: (a) surface and (b) bulk lattices for the normal phase, and (c) the bulk reciprocal lattice for the reconstructed CDW phase.

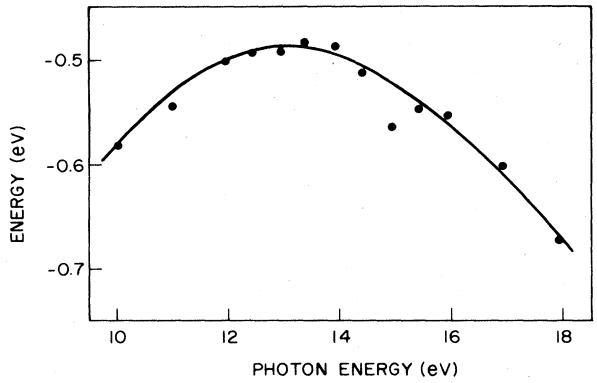

FIG. 3. Measured dispersion of the uppermost Se $4p$ band with photon energy at a constant value of $\mathbf{k}_{\|}=0.1$ Å^{-1} along $\bar{\Sigma}$. We associate the maximum near $\hbar\omega=$ 13 eV with final states for which $\mathbf{k}_{\perp}=0$.

where E_k is the kinetic energy of the photoelectrons (in eV), we find that the emission from the L pocket should be centered about $\theta=33.5°$ at 18 eV photon energy. Similarly, we find that features in the normal emission spectra originate in the Se $4p$ bands along the Δ axis ($\bar{\Gamma}$). The data of Fig. 1 does not show a semimetallic overlap, but this is not conclusive because the apparent separation of the p and d bands varies with photon energy. They are in fact closer in energy at 13 eV photon energy. This is because the Se $4p$ bands exhibit significant dispersion with photon energy as indicated in Fig. 3. Here the energy of the uppermost Se $4p$ band is plotted as a function of photon energy for a constant value of $\mathbf{k}_{\|}=0.1$ Å^{-1}. An extremum occurs near $\hbar\omega=13$ eV which we attribute to emission from initial states with perpendicular wave vector $|k_{\perp}|=0$ in accordance with band-structure calculations.

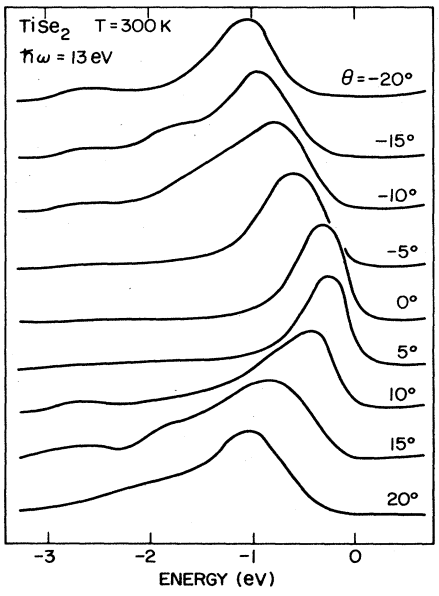

FIG. 4. Set of spectra taken at 13 eV photon energy along the $\bar{T}$ azimuth. The Se $4p$ bands display a maximum energy at $\theta=0°$, which is slightly below the lowest Ti $3d$ bands.

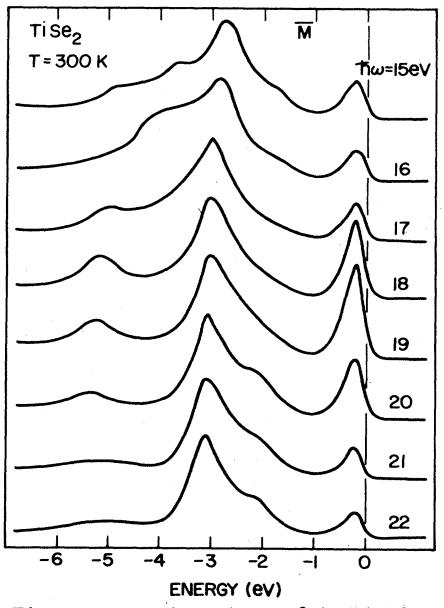

FIG. 5. Photon-energy dependence of the Ti $3d$ emission at a value of $\mathbf{k}_{\|}$ corresponding to $\bar{M}$. Local maxima in intensity are observed at 19, 26, 47, and 75 eV photon energies but very little dispersion is seen.

A set of room temperature spectra with $\hbar\omega=13$ eV appears in Fig. 4. Not coincidentally, these spectra display stronger and sharper features at the valence-band maximum than appear at higher photon energies. This observation supports the proposition that we are exciting direct $\Gamma\rightarrow\Gamma$ optical transitions at this photon energy. The low group velocities of the initial states normal to the surface at Γ will lead to narrower linewidths at such symmetry points due to reduced momentum broadening.

In principle the binding energy of the Ti $3d$ band should also demonstrate a photon-energy dependence. The observed dispersion is in fact no more than 40 meV for photon energies between 10 and 85 eV. There are strong fluctuations of the Ti $3d$ intensity with photon energy as if it were periodically dispersing toward the Fermi level, but the peak position does not change accordingly. For example, the behavior of the $3d$ emission for photon energies near $\hbar\omega=19$ eV is shown in Fig. 5. We conclude that the proximity of the Fermi level and the finite experimental resolution conceal the actual $3d$ dispersion and to some extent limit the accuracy to which its energy can be determined. The fittings of our data yield a minimum energy of -0.23 eV. When the Fermi function is folded into the fitting procedure, the algorithm returns values with more photon-energy dependence but the same apparent minimum. Maxima in $3d$ intensity occur at $\hbar\omega=$ 19, 26, 47, and 75 eV. We associate these maxima with emission from initial states near the calculated $3d$-band minimum at the L point. We place the Ti $3d$ energy minimum at -0.23 eV. Because of the Fermi-level-related effects mentioned above, we estimate a larger uncertainty toward higher energy ($+0.10$ eV) than toward lower energy (-0.05 eV).

The Se $4p$ peak in the normal emission spectrum of Fig.

4 is centered at -0.36 eV. However, if we assume that this peak is comprised of two unresolved peaks separated by 0.14 eV, the uppermost valence band might be as high as -0.29 eV. (The source of the 0.14 eV estimate of the splitting will become apparent later in this paper.) This is our best estimate of the absolute valence-band maximum. Since the conduction-band minimum is located at -0.23 eV, $TiSe_2$ appears to us to be a semiconductor at room temperature with a gap of 0.06 eV. Experimental uncertainties leave open the possibility of a slight overlap, but our findings contradict the results of Chen *et al.*[16] and Bachrach *et al.*,[15] both of which report substantial semimetallic overlaps at room temperature.

Before turning to the low-temperature data we wish to comment on the angular dependence of the Ti $3d$ emission. The angular profiles of the $3d$ intensity are essentially Gaussian. Sharp intensity drops at the Fermi-level crossing angle are not seen. Momentum broadening of the angular distribution might account for some of the rounding of the angular profile. The full width at half maximum of the filled d-band pockets in our samples is about 0.2 Å^{-1} along $\bar{\Sigma}$ and 0.1 Å^{-1} in the perpendicular direction. Therefore the three L pockets of Ti $3d$ electrons fill about 1% of the first Brillouin zone as mentioned in Sec. II. The extent of this band filling is unchanged at 77 K.

IV. ARPES OF THE CDW STATE

When the $TiSe_2$ sample is cooled to 77 K a marked decrease in the linewidths of the Se $4p$ bands is observed, particularly in the 10—15 eV photon-energy range. For example, a series of low-temperature spectra is shown in Fig. 6 for $\hbar\omega = 13$ eV. In contrast to the room temperature data of Fig. 4, it is possible to resolve two Se $4p$ bands with different effective masses in the off-normal spectra of Fig. 6. Near normal emission these bands cannot be resolved. In part this is due to a loss of intensity, especially of the upper band, near $\theta = 0$ which does not occur in the corresponding spectra of Fig. 4. The narrowing of the photoemission peaks we attribute to temperature-dependent momentum broadening. However, the loss of intensity at $\mathbf{k}_{||} = 0$ appears to be directly related to the formation of the charge density wave.

The simplicity of the dispersions and sharpness of the peaks make possible a very precise determination of the effective masses and energies of the two bands visible in Fig. 6. The dispersions of these bands are plotted in Fig. 7 along with those of similar data taken at 12 and 14 eV photon energies. There is negligible $\mathbf{k}_{\perp}$ dispersion in this narrow photon-energy range, and the data fall along two well-defined bands. The Lorentzian widths of the photoemission peaks, as determined by the peak-fitting algorithm, increase systematically from roughly 0.3 eV near $\mathbf{k}_{||} = 0$ to 0.8 eV near the zone edge. The binding energies determined by the fitting procedure should be accurate to about 30 meV. The least-squares method was used to fit the points in Fig. 7 to two sine functions of $|\mathbf{k}_{||}|$ with the periodicity of the reciprocal lattice. This fitting provides a very accurate estimate of the two p-band maxima if the bands are in fact sinusoidal. The upper sine curve reaches a maximum at -0.26 eV and the splitting between the two maxima is 0.14 eV. The effective masses of the two bands are found to be nearly isotropic along the layer directions. At $\mathbf{k}_{||} = 0$ they are -0.44 and -0.23 electron mass units $\pm 5\%$ for the upper and lower bands, respectively.

The effects of cooling to 77 K upon the Ti $3d$ peaks are very modest. The binding energy is increased by 0.01 to -0.24 eV but the linewidths and areas at $\bar{M}$ are essential-

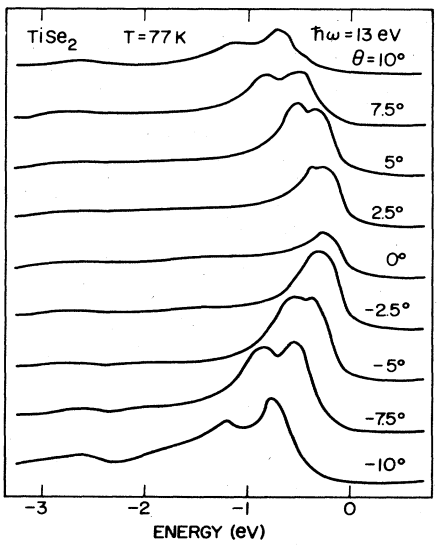

FIG. 6. Low-temperature spectra showing two well-resolved Se $4p$ bands, both of which lose intensity at $\theta = 0°$. The dispersion of these bands appears in Fig. 7.

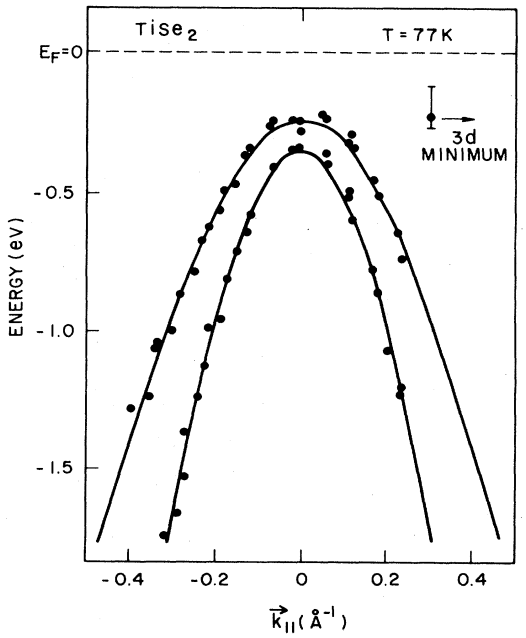

FIG. 7. Dispersion of the Se $4p$ bands in $TiSe_2$ at 77 K. Sinusoidal curves are drawn through the data as discussed in the text. Data taken at 12, 13, and 14 eV photon energy are included.

ly identical at 77 and 300 K. We conclude from the sinusoidal fit to the data that $TiSe_2$ also has a small semiconductor gap in the CDW phase. The magnitude of this apparent gap is reduced with respect to the room-temperature result principally due to an upward shift of the Se 4p bands at low temperature.

V. DISCUSSION

The relative positions of the p and d bands determine the strength of their interaction. Suzuki *et al.* have calculated the band structure of $TiSe_2$ in the p-d interaction region under the assumption of a 0.2-eV p-d overlap without any interaction.[6] They report that the electron-lattice coupled interaction between the p and d bands in the CDW phase opens gaps of 0.2 eV about the center of the Brillouin zone. The data in Figs. 6 and 7 rule out such a large gap, but smaller deviations from sinusoidal dispersion might be present.

The absence of the large predicted gap does not imply that the p-d interaction is negligible in the CDW phase. The presence of the CDW superlattice can be observed directly as an eightfold contraction of the Brillouin zone in the low temperature phase. The superlattice causes the L, A, and M symmetry points of the normal reciprocal lattice to become equivalent to Γ points of the smaller Brillouin zone of the CDW phase as illustrated in Fig. 2. These points are all connected by the new Fourier components of the superlattice crystal potential. In practice the folding down of the band structure need have only weak effects upon the ARPES spectra, because the perturbation of the crystal potential is relatively small. Nevertheless, we do see such an effect in Fig. 8. There, a distinct band of peaks exhibiting a negative effective mass can be seen within 1 eV of E_F, with both an energy and

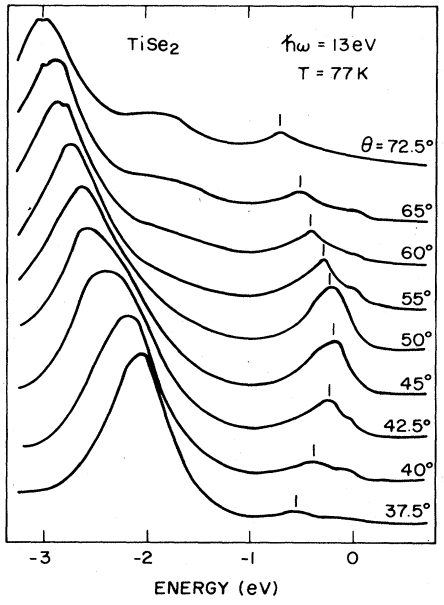

FIG. 8. Se 4p band which appears at $\overline{M}$ of the undistorted lattice due to the folding of $\overline{\Gamma}$ into this point by the CDW superlattice.

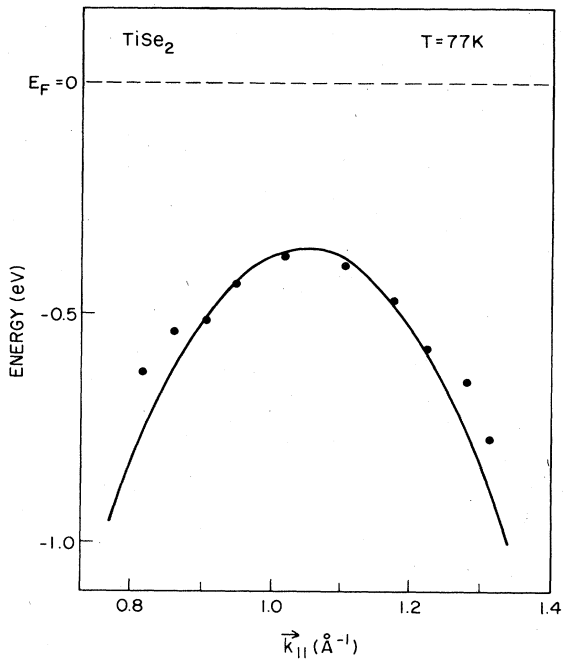

FIG. 9. Dispersion of the peaks in Fig. 8. The sinusoidal curve drawn through the data has the same effective mass as the upper curve in Fig. 7.

intensity maximum near $\theta=50°$. The dispersion of this band is plotted in Fig. 9. It forms a partial band about $|\mathbf{k}_{||}|=1.0$ Å^{-1}. Its effective mass and binding energy clearly identify it as a Se 4p band similar to those at $\mathbf{k}_{||}=0$ rather than as a Ti 3d band. (Because $\mathbf{k}_{\perp}$ is different, the mass and energy are slightly different.) Its appearance at a wave vector corresponding to the zone boundary of the normal phase can only be explained by the folding of the band structure induced by the CDW. The folded Se 4p bands are seen at $\overline{M}$ over a wide range of photon energies in the CDW phase, often as a shoulder on the low binding energy side of an intense Ti 3d peak.

If $TiSe_2$ is intrinsically a semiconductor, good quality stoichiometric crystals will have a conduction band which is essentially unoccupied except for thermally excited electrons. An earlier ARPES study[8] by one of the present authors apparently involved more nearly stoichiometric samples than the current experiment. Those samples showed no d-band peak near $\overline{M}$ at room temperature (see Fig. 10), but at 95 K a peak appears near -0.5 eV. The current results suggest that this low-temperature peak is derived from the valence band maximum rather than the conduction band. The published spectra in Ref. 8 also suggest a negative effective mass for this peak. The band folding therefore seems to be a stoichiometry independent effect. The folded Se 4p band at $\overline{M}$ might account for reports of semimetallic overlaps in $TiSe_2$ in earlier ARPES experiments.

Only the states comprising the valence band maximum show a doubled periodicity. To explain this selective effect we propose that the valence band is hybridizing with Ti 3d states only near Γ. By taking on appreciable 3d

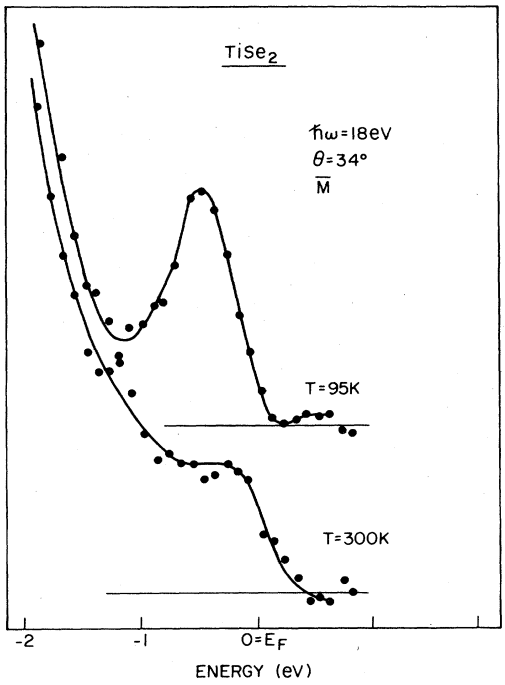

FIG. 10. Temperature-dependent $\bar{M}$ spectra taken from Ref. 8. The d bands are very weak in these nearly stoichiometric samples. The low-temperature peak is apparently the zone-folded valence-band peak.

character this band will couple more strongly to the same $\bar{M}$ final states as do the Ti $3d$ bands. The CDW therefore leads to a selective transfer of the normal emission intensity to the $\bar{M}$ points. Apparently both p-d hybridization and the extra reciprocal lattice vectors of the CDW phase are necessary to account for these temperature-dependent effects.

The temperature dependence of the spectral linewidths is not localized in energy or wave vector, and therefore has a more general origin. Photoemission linewidths are usually determined by electron and hole lifetimes and by momentum broadening. These effects should be weakly temperature dependent unless they are dominated by phonon-scattering processes. The broadening due to hole lifetimes should tend to zero for initial states near the Fermi level, yet temperature dependent effects in our spectra are very strong near E_F. If the final-state electron lifetimes decrease with temperature, the photoyield should vary along with the electron escape depth; this effect is not seen. Instead, we suggest that the temperature dependence arises from momentum broadening perpendicular to the surface. Owing to its layer structure the longitudinal-acoustic phonon modes in $TiSe_2$ are fairly low in energy along the interlayer direction. The uncertainty of the perpendicular wave vector, $\Delta k_\perp$, in the photoemission process could be influenced strongly by scattering from a temperature-dependent population of such phonons. Since both band structure calculations and our results show that there is substantial dispersion along $\mathbf{k}_\perp$ and since Γ and A are separated by only 0.52 Å^{-1}, this uncertainty will lead to substantial broadening of the ARPES features.

VI. CONCLUSIONS

The accurate measurements of the band structure in the p-d interaction region of $TiSe_2$ which we present herein should help in the refinement of the microscopic theory of the charge-density-wave phase transition. The relative p-d band positions determine not only the strength of their interaction, but also the volume of k space over which they can interact. The substantial semimetallic overlap suggested by some previous experimental and theoretical studies is not supported by our results. Nonetheless, the Se $4p$ and Ti $3d$ bands do have a significant interaction. This is suggested by the appearance of a new, presumably hybridized $4p$ band at $\bar{M}$ and by the possible slight repulsion of the p and d bands at $\bar{\Gamma}$ and the weakening of the p-band maximum at 77 K. The observation of the increased periodicity of parts of the electronic band structure below the phase transition temperature is an interesting demonstration of what was recently only a theoretical construction. The narrowing of the linewidths at low temperatures is an apparently fortuitous consequence of reduced phonon scattering which makes possible the accurate measurements we have reported.

ACKNOWLEDGMENTS

We wish to thank F. J. DiSalvo for providing the samples used in this experiment. This work was performed at the National Synchrotron Light Source which is supported by the U. S. Department of Energy, Division of Materials Sciences and Division of Chemical Sciences.

*Present address: Bell Communications Research, 600 Mountain Avenue, Murray Hill, NJ 07974.

[1]F. J. DiSalvo, D. E. Moncton, and J. V. Waszczak, Phys Rev. B **14**, 4321 (1976).
[2]J. A. Wilson, Solid State Commun. **22**, 551 (1976).
[3]H. P. Hughes, J. Phys. C **10**, L319 (1977).
[4]Y. Yoshida and K. Motizuki, J. Phys. Soc. Jpn. **49**, 898 (1980); **51**, 2107 (1982); K. Motizuki, N. Suzuki, and Y. Takoaka, Solid State Commun. **46**, 995 (1981)
[5]A. Zunger and A. J. Freeman, Phys. Rev. B **17**, 1839 (1978).
[6]N. Suzuki, A. Yamamoto and K. Motizuki, Solid State Commun. **49**, 1039 (1984).
[7]G. Margaritondo, C. M. Bertoni, J. H. Weaver, F. Lévy, N. G. Stoffel, and A. D. Katnani, Phys. Rev. B **23**, 3765 (1981).
[8]N. G. Stoffel, F. Lévy, C. M. Bertoni, and G. Margaritondo, Solid State Commun. **41**, 53 (1982).
[9]O. Anderson, G. Karschnick, R. Mahzke, and M. Skibowski, Solid State Commun. **53**, 339 (1985).
[10]J. H. Gaby, B. DeLong, F. C. Brown, R. Kirby, and F. Lévy, Solid State Commun. **39**, 1167 (1981).
[11]R. W. White and G. Lucousky, Nuovo Cimento B **38**, 280 (1977).

[12]H. Isomäki, J. von Boehm, and P. Krusius, J. Phys. C **12**, 3239 (1979).
[13]G. A. Benesh, A. M. Wooley, and Cyrus Umrigar, J. Phys. C **18**, 1595 (1985).
[14]J. von Boehm and H. M. Isomäki, J. Phys. C **15**, L733 (1982).
[15]R. Z. Bachrach, M. Skibowski, and F. C. Brown, Phys. Rev. Lett. **37**, 40 (1976).
[16]C. H. Chen, W. Fabian, F. C. Brown, K. C. Woo, B. Davies, and B. DeLong, Phys. Rev. B **21**, 615 (1980)
[17]M. M. Traum, G. Margaritondo, N. V. Smith, J. E. Rowe, and F. J. DiSalvo, Phys. Rev. B **17**, 1836 (1978).
[18]P. Thiry, P. A. Bennett, S. D. Kevan, and N. V. Smith, Nucl. Instrum. Methods (to be published).
[19]S. D. Kevan, Rev. Sci. Instrum. **54**, 1441 (1983).